Functional Materials Letters
Vol. 3, No. 4 (2010) 253–257

DOI: 10.1142/S1793604710001354

World Scientific
www.worldscientific.com

MICROWAVE DIELECTRIC PROPERTIES AND RAMAN SPECTROSCOPY OF SCHEELITE SOLID SOLUTION $[(Li_{0.5}Bi_{0.5})_{1-x}Ca_x]MoO_4$ CERAMICS WITH ULTRA-LOW SINTERING TEMPERATURES

DI ZHOU*, HONG WANG, QIU-PING WANG, XIN-GUANG WU,
JING GUO, GAO-QUN ZHANG, LI SHUI and XI YAO
Electronic Materials Research Laboratory
Key Laboratory of the Ministry of Education
Xi'an Jiaotong University, Xi'an, Shaanxi, 710049, China
**zhoudi1220@gmail.com*

CLIVE A. RANDALL
Center for Dielectric Studies, Materials Research Institute
The Pennsylvania State University, University Park, PA 16802, USA

LI-XIA PANG
Micro-Optoelectronic Systems Laboratories, Xi'an Technological University
Xi'an, Shaanxi, 710032, China

HAN-CHEN LIU
School of Science, Xi'an Polytechnic University
Xi'an, Shaanxi, 710048, China

Received 15 July 2010; Revised 29 September 2010

A Scheelite solid solution was formed based on $[(Li_{0.5}Bi_{0.5})_{1-x}Ca_x]MoO_4$ ceramics and prepared via a solid state reaction method in the range $0.0 \leq x \leq 1.0$. High performance microwave dielectric properties were obtained in the $[(Li_{0.5}Bi_{0.5})_{0.15}Ca_{0.85}]MoO_4$ ceramic sintered at 760°C with a relative permittivity of 14.1, a Qf value of 24,000 GHz (at 10.0 GHz), and a temperature coefficient value of +10.7 ppm/°C and the $[(Li_{0.5}Bi_{0.5})_{0.1}Ca_{0.9}]MoO_4$ ceramic sintered at 850°C with a relative permittivity of 12.7, a Qf value of 41,300 GHz (at 10.3 GHz), and a temperature coefficient value of −16.5 ppm/°C. X-ray diffraction, Raman spectroscopy and the classical damped oscillator model were applied to study the relationship between the microwave dielectric properties and structures.

Keywords: Microwave dielectric ceramic; low temperature co-fired ceramic; Scheelite solid solution.

As potential candidate materials for applications such as dielectric resonators, filters, dielectric waveguides, microstripline substrates, and also in all dielectric metamaterials, microwave dielectrics require a range of dielectric permittivities, high Qf values (Qf = resonant frequency/dielectric loss), and a near zero temperature coefficient of resonant frequency (TCF ≈ 0 ppm/°C).[1] In order to fabricate microwave devices with small size and high integration via a low temperature co-fired ceramic technology (LTCC), microwave dielectrics must have low sintering temperatures and chemical compatibility with high conductive metal electrodes.[2] Searching for new high performance microwave dielectrics with an intrinsic low sintering temperatures has attracted more and more attention in the recent ten years.[1–3] In our previous work, the $(Li_{0.5}Bi_{0.5})MoO_4$ Scheelite materials were found to possess a sintering temperature (ST) around 560°C, a relative permittivity, ε_r of 44.4, a Qf value of 3200 GHz and a large positive TCF ∼ +245 ppm/°C.[4] The similar Scheelite structure $CaMoO_4$ ceramic has a large negative TCF around −57 ppm/°C and microwave dielectric properties ($\varepsilon_r \approx 10.8$, Qf ≈ 89,700 GHz, ST around 1100°C) as reported by Choi

*Corresponding Author.

et al.[5] These two microwave dielectrics have opposite TCFs but the same crystal structure and therefore offer a possibility to fabricate a solid solution with near zero TCF.

Proportionate amounts of reagent-grade starting materials were prepared by the traditional mixed-oxide solid state route according to $[(Li_{0.5}Bi_{0.5})_{1-x}Ca_x]MoO_4$ compositions ($x = 0.0, 0.2, 0.4, 0.6, 0.7, 0.8, 0.85, 0.9$ and 1.0) to form single phase powders. Dense monolithic samples were obtained via sintering. Phase identification was made using an X-ray diffraction (XRD) (Scintag PADV and X2 diffractometers, ScintagInc., Cupertino, CA) with Cu Kα radiation ($\lambda = 1.54$ Å). Prior to examination sintered pellets were crushed in a mortar and pestle to become powder. Using a Raman spectrometer (inVia, Renishaw, England) excited by an Ar^+ laser (514.5 nm) at room temperature various spectra are obtained. The dielectric properties were measured at microwave frequency by the post-resonator method as suggested by Hakki and Coleman with a network analyzer (HP8510 Network Analyzer, Agilent, Hewlett-Packard). The temperature coefficient of resonant frequency (TCF) was determined using a zero thermal expansion cavity with programmable temperature chamber (Delta 9023, Delta Design, Poway, CA) in the temperature range of 25–85°C. The TCF was calculated by the following formula:

$$\tau_f = \frac{f_{85} - f_{25}}{f_{25} \times (85 - 25)} \times 10^6. \quad (1)$$

where f_{85} and f_{25} were the $TE_{01\delta}$ resonant frequencies at 85°C and 25°C, respectively.

The room temperature X-ray diffraction patterns for $[(Li_{0.5}Bi_{0.5})_{1-x}Ca_x]MoO_4$ ($0.0 \le x \le 1.0$) ceramics sintered at optimal temperatures are shown in Fig. 1. The general formula for Scheelite structure is ideally $AMoO_4$ with space group $I4_1/a$ (No. 88).[6] (The schematic illustration of the crystal structure can be found in Ref. 7) The pure $(Li_{0.5}Bi_{0.5})MoO_4$ and its defective non-stoichiometric ionic compensation $(Li_{0.5-3x}Bi_{0.5+x}\varphi_{2x})MoO_4$, where x is smaller than 0.08 and φ an A site vacancy, can form a pure Scheelite structure at around 500°C as previously reported by Klevtsov *et al*.,[8] Sleight *et al*.,[9] Zhou *et al*.[4] As shown in Fig. 1, all the XRD peaks can be indexed as a pure Scheelite phase, which is consistent with a complete Scheelite solid solution being formed in the range $0.0 \le x \le 1.0$. As the x value increases from 0.0 to 1.0, we note that the (1 0 1) peak becomes systematically stronger and this may be associated with a disordering of $(Li_{0.5}Bi_{0.5})$ replacing Ca on the A site. Although $(Li_{0.5}Bi_{0.5})MoO_4$ can retain the tetragonal symmetry at room temperature, some distortions can lead to it to tetragonal $I\bar{4}$ (No. 82) symmetry.[10] It was reported that a few very weak reflections, which were forbidden for the $I4_1/a$ space group, can fit the $I\bar{4}$ symmetry well.[11] However, it was also believed that the slightly distorted Scheelite structure with space group $I\bar{4}$ is probably due to non-stoichiometry.[12] In any case, the

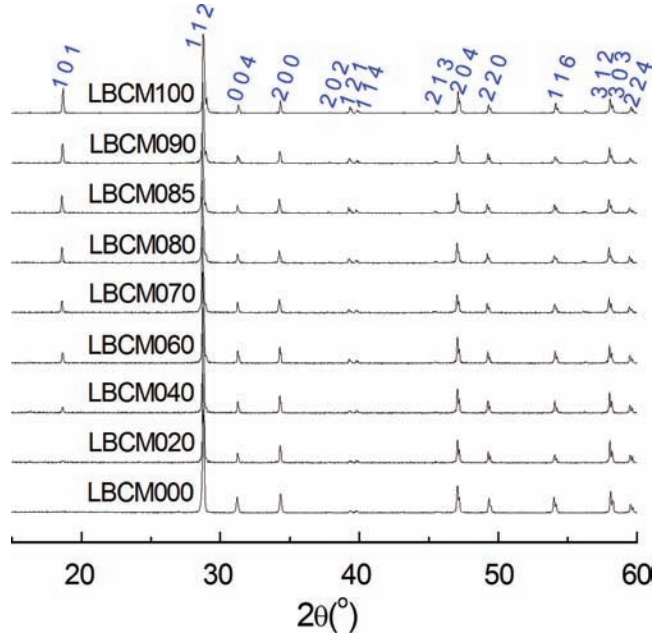

Fig. 1. XRD patterns of Scheelite solid solution $[(Li_{0.5}Bi_{0.5})_{1-x}Ca_x]MoO_4$ ($0.0 \le x \le 1.0$) ceramics.

Scheelite structure with $I4_1/a$ and $I\bar{4}$ symmetries are very similar to each other. The main difference is that Li^+ and Bi^{3+} cations randomly take the equivalent site in the $I4_1/a$ symmetry with the same occupancy factor 50%. Whereas for $I\bar{4}$ symmetry there are two non-equivalent lattice sites, 2*d* and 2*b*, both with local symmetry S_4, and with different occupancy factors, 55%Bi + 45%Li and 45%Bi + 55%Li for 2*d* and 2*b* sites in $I\bar{4}$ symmetry.[13]

Figure 2 shows the room-temperature Raman spectra of $(Li_{0.5}Bi_{0.5})_{1-x}Ca_x]MoO_4$ ($0.0 \le x \le 1.0$) ceramics. The $CaMoO_4$ has two chemical units in one unit cell and belongs to the C_{4h}^6 point group. Group theory predicts that there are 26 different vibrations in $CaMoO_4$ as following:

$$\Gamma = 3A_g + 5A_u + 5B_g + 3B_u + 5E_g + 5E_u \quad (2)$$

Among them $3A_g$, $5B_g$ and $5E_g$ are the Raman active modes. It was reported that the vibrations of $AMoO_4$ can be classified into two groups: internal and external modes.[14] The internal modes belong to the vibrations inside $(MoO_4)_2$ molecular units of which the centers of mass are stationary ($> 300\,cm^{-1}$). The external modes are lattice phonons which corresponds to the motion of A^{2+} cations and the rigid molecular units ($< 300\,cm^{-1}$).

As shown in Fig. 2, eight Raman peaks are observed, among which the peaks at $142.4\,cm^{-1}$ (E_g) and $204.1\,cm^{-1}$ (A_g) belong to the external modes, and peaks at $322.8\,cm^{-1}$ (E_g), $391.9\,cm^{-1}$ (B_g), $793.8\,cm^{-1}$ (E_g), $847.9\,cm^{-1}$ (B_g) and $878.8\,cm^{-1}$ (A_g) belong to the internal modes. Each vibration mode is in agreement with Raman vibrations analyzed by other researchers.[14] As the x value decreases, all the

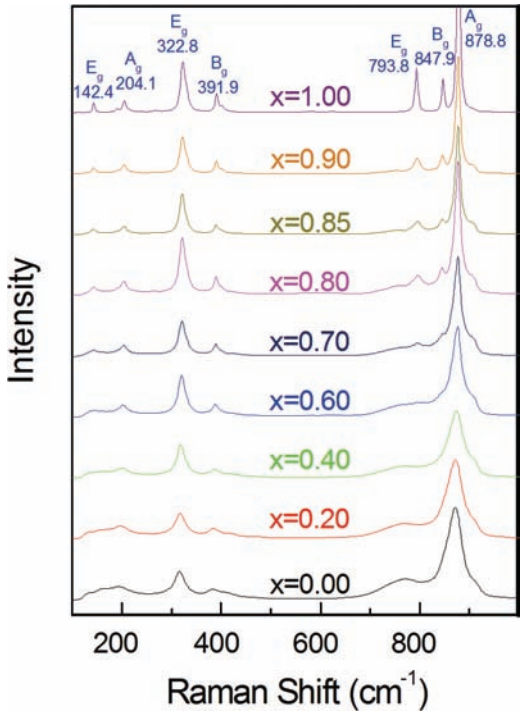

Fig. 2. Raman spectroscopy of $[(Li_{0.5}Bi_{0.5})_{1-x}Ca_x]MoO_4$ ($0.0 \leq x \leq 1.0$).

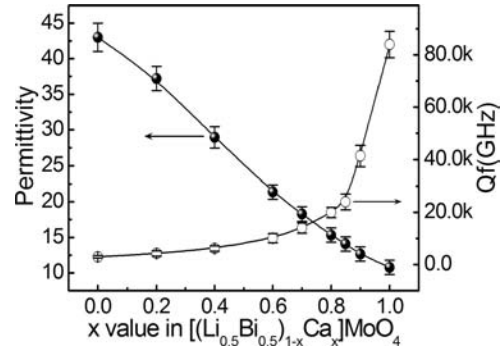

(a)

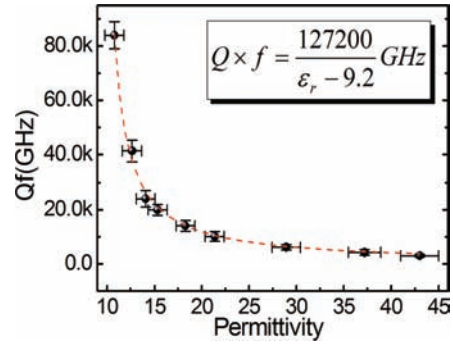

(b)

Fig. 3. Microwave dielectric relative permittivity and Qf values of $[(Li_{0.5}Bi_{0.5})_{1-x}Ca_x]MoO_4$ ceramics as a function of x value (a), and Qf values as a function of relative permittivity (b) dash fitting line was calculated using a reciprocal function.

Raman bands become weak and broaden, meanwhile many other weak modes appear and the overlapping becomes serious. For $(Li_{0.5}Bi_{0.5})MoO_4$, more Raman active modes (weak and overlapping) are observed than that of the simple Scheelites and the vibrational spectra appears to be more sensitive to short-range order than X-ray powder pattern which gives information on a random distribution of the atoms in the unit cell. The band width of the two strongest bands A_g-878 and E_g-622 are much larger than that of $CaMoO_4$, which indicates the $(Li_{0.5}Bi_{0.5})$ tend to a strong disordered arrangement on the A site in the Scheelite structure. For the other differences, Hanuza[15] assumed that there exists evidence for some short-range order most likely caused by the different arrangement of Li and Bi ions. When replacing Ca^{2+} ions in crystal lattice of $CaMoO_4$, Bi^{3+} and Li^+ can form Bi–Li–Bi–Li, for which cationic sequence the MO_4^{2-} ions occupy two nonequivalent sites, or Bi–Bi–Li–Li layers perpendicular to c axis, for which cationic sequence the MO_4^{2-} ions occupy four nonequivalent positions. This assumption has some similarity with the situation in $I\bar{4}$ symmetry. When $I\bar{4}$ symmetry is considered, the Bi^{3+} and Li^+ cations statistically occupy two positions with different occupancy factors.[12–15] The different positions of the Li^+ and Bi^{3+} ions can change the coordination number of atoms which form the crystal. This means that although Li^+ and Bi^{3+} cations are short-range ordered, their local distributions are random. So the structure exhibits local statistical deviations in the ordering of the cationic layers. This is possibly a reason for why the Raman spectra of $(Li_{0.5}Bi_{0.5})MoO_4$ crystals have a continuum character and consist of broad overlapping bands.

Microwave relative permittivity, Qf values of $[(Li_{0.5}Bi_{0.5})_{1-x}Ca_x]MoO_4$ ($0.0 \leq x \leq 1.0$) ceramics measured as a function of x value and their relationship are shown in Fig. 3. As x value increases from 0.0 to 1.0, the microwave relative permittivity decreases linearly from 44 to 10.8 and this is due to the smaller ionic polarizability for Ca^{2+} (3.16 Å^3) than that for $(Li_{0.5}Bi_{0.5})^{2+}$ (3.66 Å^3).[16] Meanwhile, the Qf value increases from 3200 to 84,000 GHz. Usually the microwave dielectric loss includes two parts: intrinsic loss caused by absorptions of phonon oscillation and extrinsic loss caused by universal defect (impurities, substitution, grain boundaries, grain morphology and shape, secondary phase, pores, etc.).[16] Considering the larger polarizability for $(Li_{0.5}Bi_{0.5})^{2+}$ than Ca^{2+}, it can be deduced that the contribution to microwave relative permittivity from $(Li_{0.5}Bi_{0.5})^{2+}$, polarization is larger than that of Ca^{2+} and the oscillation of $(Li_{0.5}Bi_{0.5})^{2+}$ is also stronger than that of Ca^{2+} in the Scheelite structure. Hence substitution of Ca^{2+} increases the Qf values of $[(Li_{0.5}Bi_{0.5})_{1-x}Ca_x]MoO_4$ ceramics. The intrinsic Q sets the upper limit for a pure defect-free single crystal

and can be quantitatively described by the well-known classical damped oscillator model in IR frequency range.[18] In this model, a roughly reciprocal relationship between Qf and the dielectric constant could be obtained as following:

$$\varepsilon^*(\omega) - \varepsilon(\infty) = \frac{(ze)^2/mV\varepsilon_0}{\omega_T^2 - \omega^2 - j\gamma\omega}, \tag{3}$$

where $\varepsilon^*(\omega)$ is the complex permittivity, $\varepsilon(\infty)$ is the electronic part of the static permittivity, ω_T is the transverse frequency of the polar phonon mode, γ is the damping parameter, z is the equivalent electric charge number, e is the electric charge for an electron, m is the equivalent atom weight and V is the unit volume. At microwave region, considering $\omega^2 \ll \omega_T^2$, the relationship between Qf value and relative permittivity can be obtained as following:

$$Q \times f \approx \frac{(ze)^2/mV\varepsilon_0}{2\pi\gamma \times (\varepsilon'(\omega) - \varepsilon(\infty))}. \tag{4}$$

Ignoring the slight difference in equivalent electric charge and unit volume (relative difference $< 0.3\%$), the calculated results and the parameters in Eq. (4) are shown in Fig. 3(b). This analysis demonstrates the fitting of the reciprocal relationship between relative permittivity and Qf value across the Scheelite solid solution $[(Li_{0.5}Bi_{0.5})_{1-x}Ca_x]MoO_4$ ceramics. The Raman spectra analysis, together with this model suggests that there is a larger microwave dielectric relative permittivity in $(Li_{0.5}Bi_{0.5})$-rich sample caused by the increase in Raman peaks, which corresponds in turn to more phonon oscillation modes, and likewise the larger microwave dielectric losses seems to correlate to the broadening and overlapping of more Raman peaks, which correspond to changes in the oscillator strength and the damping coefficients.

Temperature coefficients and sintering temperatures measured as a function of x value are shown in Fig. 4. TCF value shifts from $+250$ ppm/°C to -55 ppm/°C as x value increases from 0.0 to 1.0. Meanwhile, the sintering temperature increases from 560°C to around 1050°C. High performance microwave dielectric properties are obtained in the $[(Li_{0.5}Bi_{0.5})_{0.15}Ca_{0.85}]MoO_4$ ceramic sintered at 760°C with a relative permittivity of 14.1, a Qf value of 24,000 GHz (at 10.0 GHz), and a TCF value of $+10.7$ ppm/°C and the $[(Li_{0.5}Bi_{0.5})_{0.1}Ca_{0.9}]MoO_4$ ceramic sintered at 850°C with a relative permittivity of 12.7, a Qf value of 41,300 GHz (at 10.3 GHz), and a TCF value of -16.5 ppm/°C.

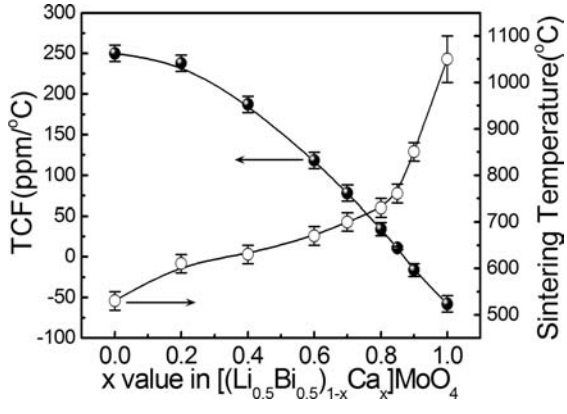

Fig. 4. Temperature coefficients and sintering temperatures of $[(Li_{0.5}Bi_{0.5})_{1-x}Ca_x]MoO_4$ $(0.0 \le x \le 1.0)$ ceramics as a function of x value.

In summary, the Scheelite phase can be formed with a complete solid solution $[(Li_{0.5}Bi_{0.5})_{1-x}Ca_x]MoO_4$. As the x value decreases, the microwave dielectric relative permittivity increases and the Qf value decreases sharply and it is inferred that this is due to the disordering and local short-range behavior with the substitution of $(Li_{0.5}Bi_{0.5})^{2+}$ for Ca^{2+} on the A site. This result corresponds very well with the classical damped oscillator model. A near zero temperature coefficient of resonant frequency can be obtained for solutions $x = 0.85$ to $x = 0.90$. This new system might be a promising candidate for the low temperature co-fired ceramic technology.

Acknowledgments

This work was supported by the National 973-project of China (2009CB623302), NSFC projects of China (10979035, 60871044, 50835007), National Project of International Science and Technology Collaboration (2009DFA51820) and the National Science Foundation I/UCRC program, as part of the Center for Dielectric Studies under Grant No. 0628817.

References

1. M. T. Sebastian and H. Jantunen, *Int. Mater. Rev.* **53**, 57 (2008).
2. M. Valant and D. Suvorov, *J. Am. Ceram. Soc.* **83**, 2721 (2000).
3. D. Zhou, H. Wang, L. X. Pang, C. A. Randall and X. Yao, *J. Am. Ceram. Soc.* **92**, 2242 (2009).
4. D. Zhou, C. A. Randall, H. Wang, L. X. Pang and X. Yao, *J. Am. Ceram. Soc.* **93**, 1096 (2010).
5. G. K. Choi, J. R. Kim, S. H. Yoon and K. S. Hong, *J. Eur. Ceram. Soc.* **27**, 3063 (2007).
6. A. W. Leight and W. J. Linn, *Ann. NY. Acad. Sci.* **272**, 22 (1976).
7. D. Zhou, C. A. Randall, H. Wang, L. X. Pang and X. Yao, *J. Am. Ceram. Soc.* **93**, 2147 (2010).
8. P. V. Klevtsov, V. A. Vinokurov and R. F. Klevtsova, *Sov. Phys. Crystallogr.* (*Engl. Transl.*) **18**, 749 (1974).
9. A. W. Sleight, K. Aykan and D. B. Rogers, *J. Solid State Chem.* **13**, 231 (1975).
10. J. Hanuza, A. Haznar, M. Maczka, A. Pietraszko, A. Lemiec, J. H. van der Maas and E. T. G. Lutz, *J. Raman Spectrosc.* **28**, 953 (1997).
11. J. Hanuza, A. Benzar, A. Haznar, M. Maczka, A. Pietraszko and J. H. van der Maas, *Vib. Spectrosc.* **12**, 25 (1996).
12. M. Maczka, E. P. Kokanyan and J. Hanuza, *J. Raman Spectrosc.* **36**, 33 (2005).

13. A. Méndez-Blas, M. Rico, V. Volkov, C. Cascales, C. Zaldo, C. Coya, A. Kling and L. C. Alves, *J. Phys.: Condens. Matter* **16**, 2139 (2004).
14. T. T. Basiev, A. A. Sobol, Y. K. Voronko and P. G. Zverev, *Optic. Mater.* **15**, 205 (2000).
15. J. Hanuza, M. Maczka and J. H. van der Maas, *J. Mol. Struct.* **348**, 349 (1995).
16. R. D. Shannon, *J. Appl. Phys.* **73**, 348 (1993).
17. H. Tamura, *Am. Ceram. Soc. Bull.* **73**, 92 (1994).
18. J. Petzelt and S. Kamba, *Mater. Chem. Phys.* **79**, 175 (2003).